

# Comparison of experimental and numerical work on three dimensional trailing edge modifications on airfoils

W. Hage\*, R. Meyer\*  
German Aerospace Center (DLR), D-10623 Berlin, Germany

M. Schatz†  
Technical University Berlin; D-10623 Berlin, Germany

## Abstract

Miniflaps at the trailing edge of airfoils (i.e., Gurney flaps) change the Kutta condition and thus produce higher lift. Unfortunately, however, the drag also increases due to the flow separation downstream of such modified trailing edges. The present work describes investigations aimed at the stabilization of the wake flow in order to achieve drag reduction and a decrease of sound generation. Using hot wire velocimetry, the existence of a tonal component could be observed in the broadband spectrum of the velocity fluctuations downstream of the Gurney flap. This points to the occurrence of a von Kármán vortex street (i.e., an absolute instability). This phenomenon persists even for turbulent boundary layers on the airfoil. Geometrical modifications of the Gurney flaps can reduce or eliminate the instability of the flow and can thus reduce or eliminate the existence of the tonal component of the velocity fluctuations of the wake. The effectiveness of trailing edge modifications like slits in Gurney flaps was investigated experimentally. These experiments were carried out with two-dimensional airfoils. The chord Reynolds number of these experiments was  $Re = 1 \times 10^6$ . At lower angles of attack where the instabilities did occur, the geometrical modifications produced an appreciable drag reduction. This drag reduction was determined directly by force measurements using a wind tunnel balance.

For a better understanding of the underlying flow physics, the unsteady flow structures in the wake of an airfoil with Gurney flap were additionally investigated by numerical simulations. These simulations were based on Reynolds-averaged Navier-Stokes methods (URANS) and Detached Eddy Simulation (DES) methods. The results from the simulation confirmed the existence of a two-dimensional vortex street. The application of Gurney-flaps with slits, however, led to more complex three-dimensional flow structures coupled with lower lift fluctuations and reduced drag.

## Nomenclature

$c$	= chord length	$S_{ij}$	= mean flow strain rate tensor
$C_D$	= drag coefficient	$St$	= Strouhal number
$C_L$	= lift coefficient	$u'$	= velocity fluctuation
$C_{L_{max}}$	= maximum lift coefficient	$\bar{u}$	= mean velocity
$C_L'$	= lift coefficient gradient	$y$	= vertical coordinate
$f_0$	= discrete frequency	$\alpha$	= angle of attack
GF	= Gurney flap	$\varepsilon_{max}$	= max. ratio of lift to drag
$h$	= trailing edge height	$\varepsilon_n$	= maximum residual in mass and momentum balance normalized by global mass flux
$h_{GF}$	= Gurney flap height	$\lambda_2$	= 2 <sup>nd</sup> Eigen value of vorticity tensor
$\Delta h_{GF}$	= effective Gurney flap height	$\varphi$	= sweep angle
$h/c$	= ratio of Gurney flap height to chord length	$\Omega_{ij}$	= mean flow rotation rate tensor
$Re$	= Reynolds number		

\* Scientist, Department of Turbulence Research, Müller-Breslau-Straße 8;

† Scientist, Herrmann Föttinger Institute for Fluid Mechanics, Müller-Breslau-Straße 8

## Introduction

For many years, the necessity of increasing the lift of airplane wings for landing and takeoff has been addressed by developing suitable flap systems. Split flaps were developed and flown as early as 1930 [1]. Particularly at high lift coefficients, split flaps are superior to simple flaps [2]. The high lift systems of today's airliners are, however, substantially more complex and exhibit retractable slats and slotted flaps (Fowler flaps). Even more effective than split flaps, where the fulcrum lies in front of the trailing edge, are strongly deflected small flaps (up to 90 °) having a fulcrum at the trailing edge. This configuration was first described by Zaparka [3] in a patent from 1935. A distinct lift increase is attained even with very small flaps of just one percent of the airfoil chord length. At the end of the 1960s the racing driver and engineer Daniel Gurney installed small fixed flaps of this kind on his vehicles (Gurney flaps). Nowadays they are used on all racing cars with wings producing downward force to improve road grip. Liebeck [4] realized the potential of this invention for airplane wings. Even with conventional flap/slat configurations, which have reached maximum performance with such designs, a further lift increase can be achieved by the additional mounting of a Gurney flap [5,6]. The Gurney flap is a fairly inconspicuous small trailing edge modification with typical dimensions of only approx. 1 % of the airfoil chord length. A further example of a trailing edge modification is the so-called "diverging trailing edge" on transonic airliner airfoils. In this the work of Henne [7] particularly may be regarded as pioneering. In the meantime, this concept has been developed for an application on airliners (McDonnell Douglas MD 11). After the acquisition of McDonnell-Douglas by Boeing divergent trailing edges were also successfully tested on a Boeing 747 [8]. With a Gurney flap the aerodynamic loading of the lower surface of the wing is increased for the same overall lift, the upper surface being thereby relieved [9,10]. As a consequence, the local supersonic Mach number on the forward part of the upper side of the airfoil is lower. This ensures weaker shock at the downstream end of that supersonic flow region and the drag is significantly reduced [7,9]. However, the design of such profiles is not trivial, as a blunt trailing edge per se causes an increase of drag. Nevertheless, for transonic airliner airfoils modified trailing edges are evidently an interesting possibility for improvements. Another important application of modified airfoil trailing edges are fluid flow machines. An increase in the output of wind turbines has already been reached using Gurney flaps [11]. The noise generation by wind-turbines is particularly critical and the separated unstable flow behind a Gurney flap does contribute unfavourably to noise generation.

First computations of the flow around a Gurney flap have been published by Sauvage [10,12] and produce qualitatively useful predictions of the time averaged flow situation. Further computational investigations that also refer only to mean quantities were done by Lee and Kroo [13]. A more detailed time resolved numerical study of the unsteady flow has been published recently by Schatz et al. [14]. The results indicated the appearance of a two-dimensional von Kármán vortex street in the wake of the Gurney flap is also coupled with lift fluctuations. Such behaviour is well-known in the wake of bluff bodies [15]. Hot wire measurements conducted in the wake of a Gurney flap also confirmed the occurrence of a vortex street his [16, 17].

In the literature however, only few references to the investigation on flow instabilities behind Gurney flaps can be found [18]. Stabilization of the wake behind cylinders or bluff bodies, and thus an elimination of the von Kármán vortex street, can be achieved using "splitter plates". These are thin plates aligned with the mean flow, which are introduced into the wake flow. Using splitter plates, a clear drag reduction can be achieved in the case of cylinders [19]. The potential benefits of using splitter plates behind Gurney flaps are obvious. In the study by Sauvage [10] the flow around a very short splitter plate is computed, albeit with an inappropriate method based only on stationary quantities. Furthermore, the application of a splitter plate behind a diverging trailing edge for the purpose of drag reduction is explicitly described in the patent specification of Allen [20].

Altogether the physical understanding of the interaction between wake instability and drag reduction are rather rudimentary in the existing literature. Our present research therefore aims to address this issue.

## Experimental Setup

Two different straight wings were investigated in the 2D airfoil test section of a wind tunnel (Fig. 1). The test section has a diameter of  $1.4 \times 2.0$  m. The maximum air speed is 40 m/s. The turbulence intensity in the wind tunnel is less than 0.2 %. The tested wing is connected to the wind tunnel balance, thereby permitting a direct force measurement of the overall air loads acting on the wing (lift, drag and pitching moment). The initial gap of 2 mm between the wing and the side wall is reduced to 0.1 mm during the measurements with a thin adhesive tape. The angle of attack is adjusted by a stepping motor with an accuracy of  $0.1^\circ$ . At the airfoil, an essentially two-dimensional flow is obtained.

The 2D flow quality was checked by flow visualizations. 85 % of the wing span were found to be completely 2D. The other 15 % are influenced by the turbulent boundary layer of the sidewalls. The measured drag with the force balance is slightly higher than that of the plain wing section drag due to induced drag components of the gap and due to the turbulent boundary layer at the side walls. The force balance has an accuracy of 0.2 % for the

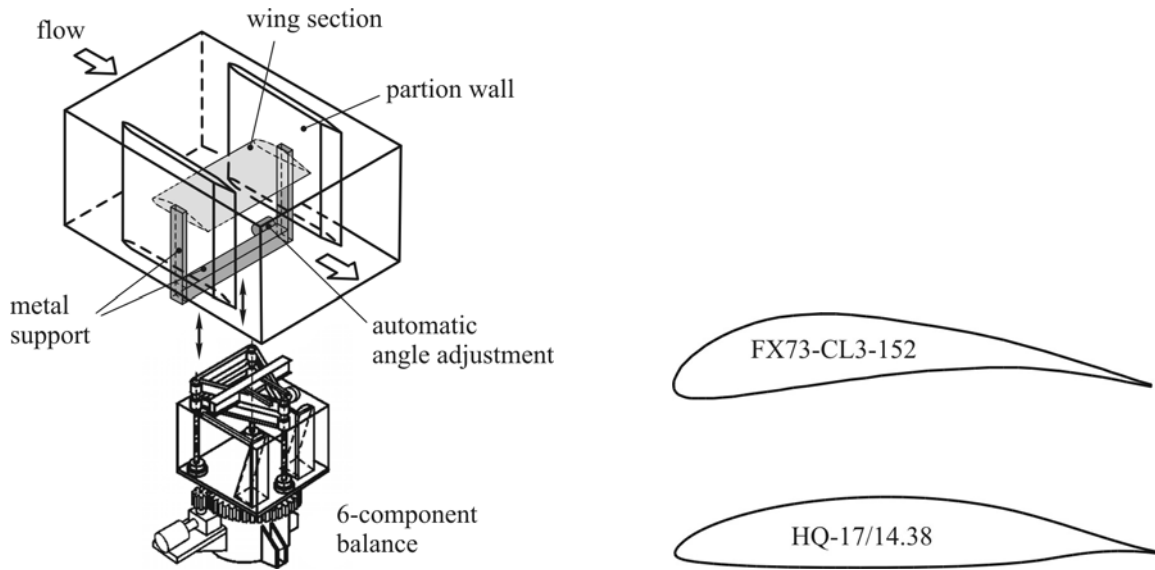


Fig. 1 left: Wind tunnel test section for two dimensional wing models; right: Investigated airfoils

lift and drag components. A more detailed description of the experimental setup and the wind tunnel is published in [21].

Two wings with a span of 1.55 m and a chord length of 0.50 m (see Fig. 1) were investigated. The airfoils have a characteristic trailing edge thickness of  $h/c = 0.33\%$ . The airfoil HQ17/14.38 shows a typical laminar glider profile with a minimal drag at moderate angles of incidence (e.g. at cruise condition). The profile was developed by Horstmann and Quast from DLR Braunschweig. This wing is particularly suitable for measurements of the smallest drag changes arising from the trailing edge modifications. The maximum lift coefficient of this airfoil is  $C_{L,max} = 1.4$ . The high lift airfoil (FX73-CL3-152) devised by Wortmann has a strong curvature and achieves a very high maximum lift coefficient of  $C_{L,max} = 2.2$ . The indicated  $C_{L,max}$  values refer to an airfoil Reynolds number of  $Re = 1 \times 10^6$ .

## Drag reduction by wake stabilization

In the separated flow downstream of a Gurney flap we expect that an absolute instability [22, 23, 24] can be observed. One well-known example of an absolute instability is the von Kármán vortex street which occurs in the wake of a cylinder. Such instabilities occur not only in laminar flows, as the classical experiments with cylinders would suggest, but they can be also observed in turbulent flows. A typical sign for an absolute instability is the occurrence of a single peak in the spectrum of the fluctuations in or near the wake. The reversed flow in the wake is a property which enhances this instability [23]. Since trailing edges of airfoils are usually not

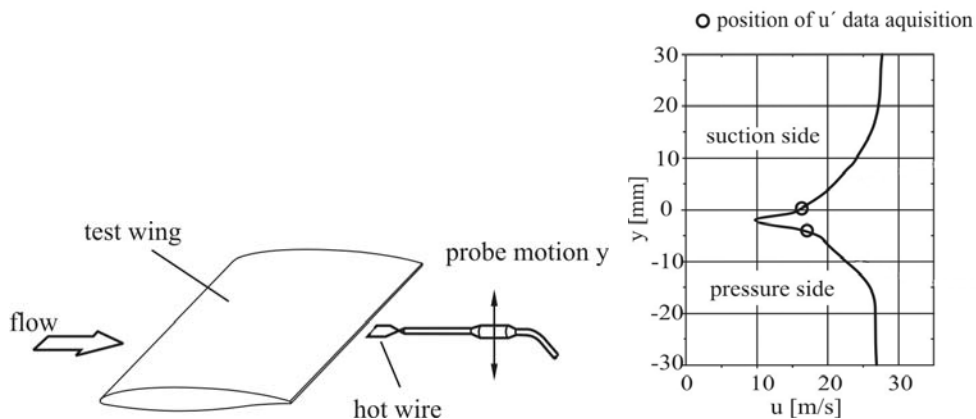


Fig. 2 left: Test arrangement for wake measurements with a hot wire; right: Mean flow  $\bar{u}$  distribution of wake of the Airfoil HQ17;  $\alpha = -1^\circ$ ,  $Re = 1.0 \times 10^6$ .

very sharp, we also expect such an absolute instability in the wake of an (even slightly) blunt trailing edge.

Our first aim was, therefore, to demonstrate experimentally, that a single frequency does exist in the fluctuations downstream of the trailing edge, and then devise trailing edge modifications to suppress those periodic fluctuations. The easiest way to measure velocity fluctuations is provided by the well-established hot wire anemometry (see Fig. 2). First, the mean flow distribution downstream of the wing was measured. In places of maximum mean velocity gradient the highest stream wise velocity fluctuations  $u'$  occurred. The  $u'$  fluctuations were collected at two locations with steep mean flow velocity gradient (see Fig. 2). The  $u'$  fluctuation signals were Fourier-analyzed and the spectra were plotted. Fig. 3 shows recorded data of the reference wing without Gurney flap. Due to the finite thickness of the trailing edge (0.33% chord) of this wing,

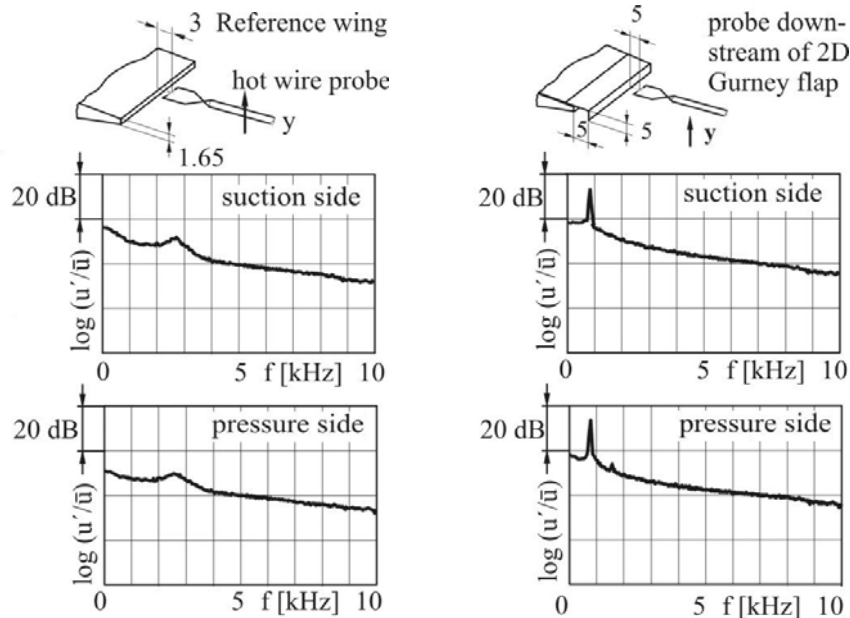


Fig. 3 Spectra of  $u'$  fluctuation of Airfoil HQ17,  $Re = 1.0 \times 10^6$ ,  $\alpha = -1^\circ$ , all dimensions in mm.  
left: Spectra of  $u'$  fluctuation of the airfoil with finite trailing edge (0.33% c);  
right: Spectra of  $u'$  fluctuation in the wake of a 2D Gurney flap with a total height of 1% c.

there is a small hump in the spectrum, signifying an (albeit weak) absolute instability, which is highlighted by its single resonance frequency  $f_0 = 2.4$  kHz. This hump vanishes for a very sharp trailing edge.

The Gurney flap height which was used throughout the investigations has a total height of  $h_{GF}/c = 1\%$  with an effective height of  $\Delta h_{GF} = 0.67\%$ , taking into account that the bluff trailing edge of the reference wing has a height of  $h/c = 0.33\%$ . The wake of a 2D Gurney flap is wider, indicating a higher drag. In addition, the  $u'$ -fluctuation levels are higher and the periodic constituent with the frequency  $f_0 = 0.8$  kHz is much stronger (see Fig. 3 right figure). Similar data was obtained if the mean flow velocity is reduced to one half of its previous value, yielding a Reynolds number of  $0.5 \times 10^6$ . As expected, the peak frequency  $f_0$  is also reduced to half of its previous value. If one calculates a Strouhal number with the frequency  $f_0$ , the Gurney flap height and the mean flow velocity, a resonance Strouhal number of  $St \approx 0.14$  is obtained. It is conceivable that other reference lengths like, e.g., the momentum loss boundary layer (or wake) thickness may be a more appropriate reference length here.

## Gurney flaps with slits

It is known from the von Kármán vortex street on cylinders, that a three-dimensional structure of the wake flow effectively suppresses the absolute instability. On a cylinder, that can be achieved by applying a helical structure on its surface (i.e., the Screwton spiral) which can be seen quite often on industrial chimneys. Obviously, this approach cannot be directly transferred to our problem. However, as it will turn out, there are various possibilities like holes or vortex generators to obtain a three-dimensional wake flow field [16]. In the present work, only slits were investigated experimentally and numerically.

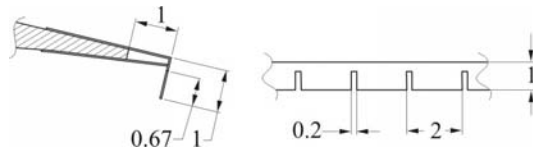


Fig. 4 Gurney flap and slit geometry, dimensions in percent chord.

The applications of slits in the Gurney flaps are shown in Fig. 4. The effect of the slits on the wake can be seen from the spectra plotted in Fig. 5. The hot wire data show clearly that the absolute wake instability (i.e., the peak in the spectrum) has almost completely vanished. Drag polars can be seen in Fig. 6, the effect of the 3D Gurney flap is visible for both examined airfoils. Table 1 shows a summary of the performance data of both airfoils. It is obvious that the additional device drag is considerably decreased by 25 %. On the other hand, the bleed air through the slits causes the Gurney flap to appear smaller, which slightly decreases the gain in lift. At higher angles of attack, however, the improvement due to the slits in the flaps is less pronounced. The hot wire data of the 2D Gurney flap (not shown here) do not exhibit any resonance either. As a matter of fact, Koch [24] has already predicted that the absolute instability disappears for strongly asymmetric wakes. Obviously, for high angles of attack, the wake of an airfoil becomes strongly asymmetric.

Therefore, the drag at high angles of attack cannot be reduced anymore by instability suppression in the wake. On the other hand, drag reduction is particularly desired at low angles of attack and, as Fig. 6 show, it is indeed achieved there. Finally, we expect that, due to the elimination of the absolute instability of the wake, also mechanical vibrations of the wing (induced by periodic changes in lift) and radiated noise are very likely to be reduced.

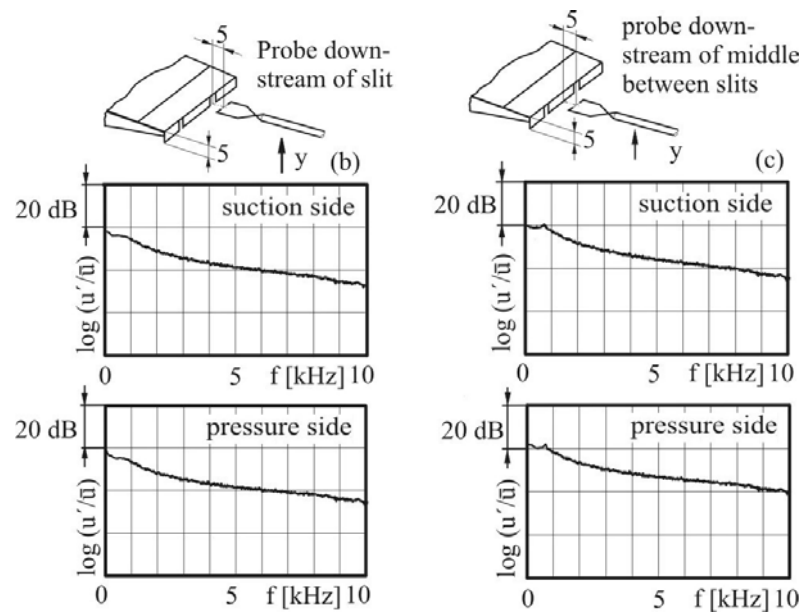


Fig. 5 Spectra of  $u'$  fluctuation of Airfoil HQ17,  $Re = 1.0 \times 10^6$ ,  $\alpha = -1^\circ$ , all dimensions in mm.  
left: Spectra of  $u'$  fluctuation downstream of a slit in a 3D-Gurney flap;  
right: Spectra of  $u'$  fluctuation downstream of middle between slits a 3D-Gurney flap.

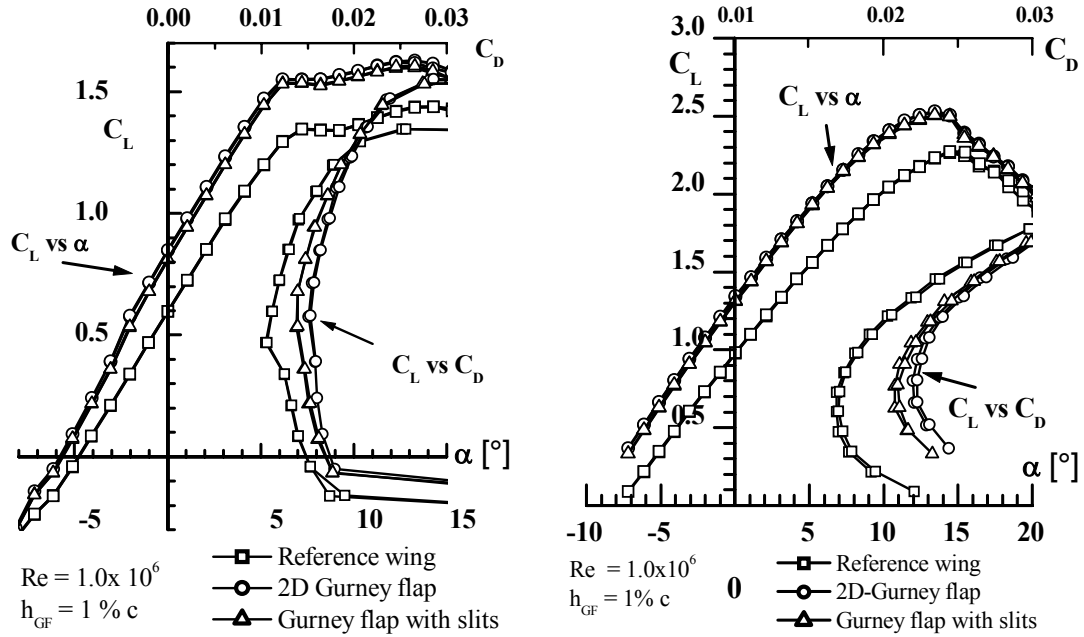


Fig. 6 left: Polar diagrams of airfoil HQ17 with a Gurney flap with slits; right: Polar diagrams of airfoil FX73 with a Gurney flap with slits.

Airfoil: HQ17, $Re = 1.0 \times 10^6$ .			
Reference wing, —□—	$C_{L \max}$	$C_{D \min}$	$\epsilon_{\max}$
2D Gurney flap —○—	1.438	0.011	69.6
3D Gurney flap with slits, —△—	1.627	0.015	63.6
	1.605	0.014	64.6
Airfoil: FX73, $Re = 1.0 \times 10^6$			
Reference wing, —□—	$C_{L \max}$	$C_{D \min}$	$\epsilon_{\max}$
2D Gurney flap —○—	2.272	0.017	61.8
3D Gurney flap with slit, —△—	2.531	0.022	56.4
	2.505	0.021	56.9

Table 1 Performance data of the Gurney flap with slits

## Numerical simulation

The unsteady flow structures in the wake are additionally investigated by numerical simulations in order to assess the details of the underlying flow physics. The applied numerical method is based on a three-dimensional incompressible finite-volume scheme to solve the Navier-Stokes equations. The method is fully implicit and of second order in space and time. Based on the SIMPLE pressure correction algorithm, a co-located storage arrangement for all quantities is applied. Convective fluxes are approximated by a third order TVD-MUSCL-scheme. In the URANS investigations, the LLR  $k-\omega$  model by Rung [25] is used which showed improved predictions of unsteady airfoil flows with large separation in former investigations [26]. Additionally, Detached Eddy Simulations (DES) have been performed which are also based on the LLR  $k-\omega$  model (for details see [14]). The DES approach offers the possibility to yield results of high resolution and physical quality with much lower numerical effort than required by Large-Eddy-Simulations.

The three-dimensional mesh around the HQ17 airfoil with a  $h_{GF}/c = 1\%$  Gurney flap consists of 40 layers of an originally 2D mesh with  $453 \times 89$  cells covering  $2h_{GF}$  in the span wise direction and has about  $1.6 \times 10^6$  nodes. The computational domain covers 7 chords upstream and 10 chords downstream of the configuration. The Gurney flap is represented by a single mesh line on both sides of which non-slip boundary conditions are applied. For the DES the same three-dimensional mesh can be applied. Further investigations cover Gurney flaps with slits that can be compared to those discussed above (Fig. 4). The same mesh can be used for 2D Gurney flaps as well as for those with slits by removing the wall boundary condition on appropriate parts of the Gurney flap to create slits. The transition positions are fixed on the suction and on the pressure side of the airfoil. A separate study of the influence of time stepping indicated that a typical time step of  $\Delta t = 0.002 c/u$  is sufficient

to obtain results independent of the temporal resolution and was used for both URANS and DES computations. At each single time step the mass and momentum balances are solved until a residual of  $\varepsilon_n < 10^{-6}$  normalized by the global mass flux is reached.

## Two-dimensional Gurney flaps

Numerical simulations of the 2D Gurney flap result in an almost completely two-dimensional flow field and therefore, at first two-dimensional URANS simulations were performed. Here, the mean lift clearly increases with the height of the Gurney flap. The relation between flap height and lift however is not linear but reaches saturation for very large Gurney flaps. The computational results show the same behaviour that was observed in the experiments before, not only for the linear part of the polar but also for higher angles of attack. Comparisons between steady and unsteady numerical simulations indicate that the lift coefficient can be predicted accurately based on steady computations whereas reliable results for the drag can only be obtained from unsteady computations [14]. Only these are able to capture the dynamics of flow structures in the wake which play an important role for the drag.

For low angles of attack, the flow structures are much more evident than at higher incidence, where interaction with other separation processes is dominating. Therefore, investigations are focused on a case with  $\alpha = 0^\circ$ . Analysis of the time depending lift coefficient shows that it can be characterized by one dominant frequency corresponding to the vortex shedding for all investigated cases. Table 2 lists the Strouhal-number, which represents the dominant shedding frequency normalized by the flap height. The fluctuation intensity  $C_L'$  is based on the RMS value of the lift coefficient. The characteristic behaviour of the predicted frequencies is similar to those measured by hot-wire anemometry when increasing flap heights the frequency decreases. At the

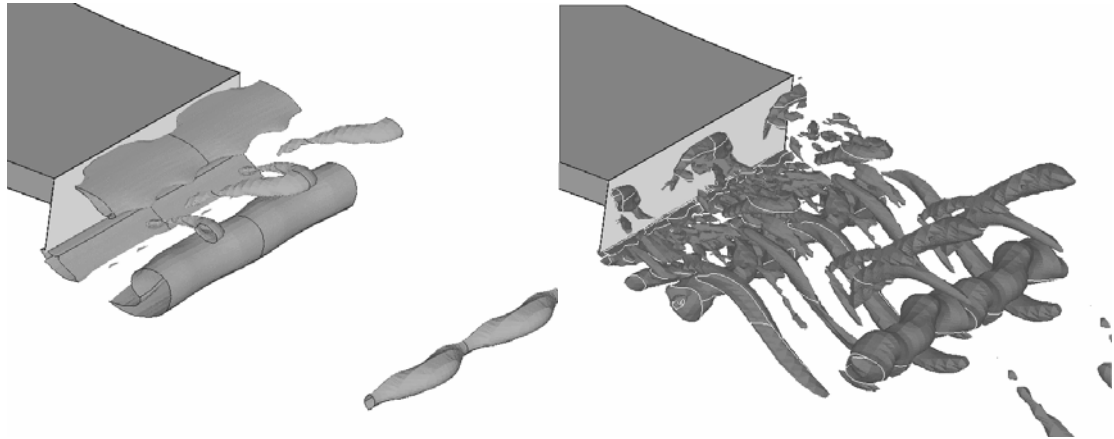


Fig. 7 Iso-surfaces of  $\lambda_2$  in the wake of a 2D Gurney flap with  $h_{GF}/c = 1\%$  computed by URANS (left figure) and DES (right figure).

same time, however, the experimental Strouhal-number increases and asymptotically reaches  $St \approx 0.18$  for very large Gurney flaps ( $h_{GF}/c > 5\%$ ). Compared to the hot-wire measurements (Fig. 3) and experiments by the authors and by Zerihan and Zhang [27] reporting  $St = 0.14$  for  $h_{GF}/c = 1\%$  the Strouhal-number is underestimated in the computations ( $St = 0.11$ ). In the case of the clean airfoil and for the smallest Gurney flap ( $h_{GF}/c = 0.5\%$ ) almost no unsteadiness can be identified in the lift coefficient and  $C_L'$  remains negligible. For larger flaps, the lift fluctuations become more eminent and grow super proportionally to the flap height in a similar manner to the extra drag induced by the Gurney flap. This behaviour is an indication that the intensity of vortex shedding characterized by  $C_L'$  is responsible for the drag augmentation. Lift and drag are determined by integration of pressure and wall shear-stress along the airfoil surface. Discrepancies to the experiments basically arise from occurring 3D effects due to the sidewalls in the experiments which are neglected in the computations.

Airfoil: HQ17	$\overline{c_L}$	$C_L'$	$\overline{c_D}$	St
clean	0.636	0.000	0.008	0.12
$h_{GF}/c=0.5$	0.709	0.000	0.008	0.10
$h_{GF}/c=1.0$	0.855	0.004	0.011	0.11
$h_{GF}/c=1.5$	0.957	0.014	0.016	0.15
$h_{GF}/c=2.0$	1.035	0.017	0.022	0.16

Table 2: Computed integral quantities and dominant frequency for  $\alpha=0^\circ$  and varying flap height.

Besides the mean quantities, the computational results also provide the unsteady behaviour of the entire flow field and especially the structures of the flow behind the Gurney flap (see Fig. 7, left figure). The figure shows iso-contours of  $\lambda_2$ , the second largest Eigen-value of a combination  $S_{ik}S_{kj}+\Omega_{ik}\Omega_{kj}$  of the strain and vorticity tensors. All negative iso-contours of  $\lambda_2$  include a local minimum of pressure and can therefore be used to identify vortices in complex flows [28].

One single principal behaviour can be observed for each flap height: Two shear layers appear that continuously separate from the top and the bottom end of the flap. After a short distance they roll up forming alternating vortices of counteracting direction of rotation which indicates the absolute instability. Although the size of typical structures depends on the flap height, the relation is not proportional; the vortices grow slower. The shape of the occurring flow structures is comparable to PIV measurements for a Gurney flap in ground effect by Zerihan and Zhang [27].

Although snapshots from URANS computations show 3D effects especially in the near wake behind the suction side, the overall flow field is characterized by the shedding of two-dimensional rolls (Fig. 7, left figure). The typical behaviour of DES is caused by the resolution of turbulent fluctuations in the LES region. Such very complex structures appear in the near wake (see Fig. 7, right figure). Compared to URANS, stronger vortices occur but these are no longer concentrated in a single dominating structure. The prediction of characteristic frequencies compared to experiments can be improved by DES.

### 3D Gurney flaps with slits

In the experiments three-dimensionally modified Gurney flaps have been shown to reduce the drag. As computational simulations of such configurations require a considerable numerical effort, only one selected version of Gurney flaps with slits is investigated here. In Fig. 8, the flow fields predicted by URANS and DES are plotted. Compared to the Gurney flap without slits, the two-dimensional rolls are weakened and irregular vortices appear instead. Even though in both the URANS and the DES results, very complex structures dominate the near wake and in particular the region downstream of the slits, vortex shedding is still visible. Again the intensity of vortices predicted by DES is larger than in the case of URANS. Compared to the strong rolls behind the 2D Gurney flap, here the smaller structures with no common orientation tend to interact and dissipate faster. They vanish without being convected far downstream. The main effect of the slits in drag reduction is based on this phenomenon. The introduction of slits leads to a drop in lift of about 5 % (Table 3). In the DES the drag can be reduced similar to the experiments predicting a reduction of mean drag by 12 % coupled with strong three-dimensionality and a significant reduction of lift fluctuation.

Airfoil: HQ17	$\overline{c_l}$	$C_l'$	$\overline{c_d}$	St
Exp. 2D Gurney flap	0.851	-	0.016	0.14
DES 2D Gurney flap	0.823	0.004	0.012	0.13
Exp. 3D Gurney flap	0.813	-	0.015	-
DES 3D Gurney flap	0.810	0.014	0.012	0.12

Table 3 Integral quantities and Strouhal number for 2D and 3D Gurney flaps computed by DES.  $\alpha = 0^\circ$ ,  $Re = 1 \times 10^6$



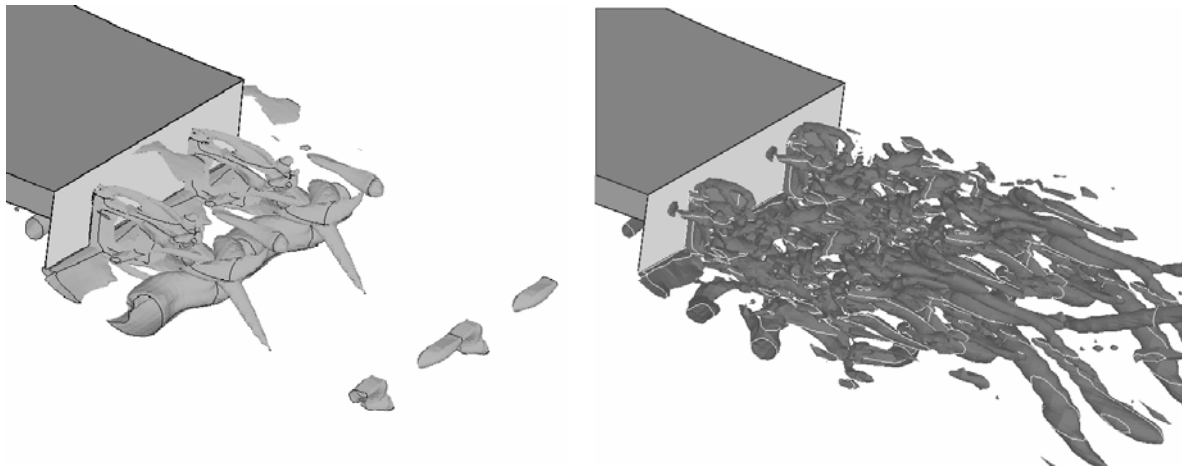


Fig. 8 Iso-surfaces of  $\lambda_2$  in the wake of a 3D Gurney flap with slits computed by a URANS (left figure) and DES (right figure).

## Conclusions

### Experiments:

The drag reduction produced by 3D Gurney flaps has been shown to be effective with the investigated airfoils. The drag reduction is clearly shown by force measurements. The impact of the 3D modification of the Gurney flaps on the lift is relatively small. The spectrum of the velocity fluctuations shows a discrete frequency with a two-dimensional Gurney flap. When using a three-dimensional Gurney flap, the amplitude of this discrete frequency is clearly reduced. On airfoils HQ17 and FX73, the drag reduction is apparent over a larger range of angle-of-attack. In general, periodic flow separation can be found on wings with an almost two-dimensional flow field (small or no sweep angle) and an airfoil profile with approximately the same upper and lower boundary layer thicknesses. This case can be influenced effectively with the three-dimensional Gurney flap configurations.

### Computations:

Unsteady computations show that the Gurney flap enhances the mean lift coefficient similar to the experimental results. Additionally, a significant augmentation of drag alongside the higher lift is closely coupled to the appearance of unsteady two-dimensional flow structures in the wake. The numerical simulations show dominant structures that strongly depend on the flap height. Results that are in satisfying agreement with experiments can be obtained using the LLR  $k-\omega$  turbulence model as well as by computations based on a DES. In the case of URANS, very regular structures appear in the wake whereas the DES predicts more complex flow structures which are nevertheless dominated by the same vortex shedding mechanism. Three-dimensional slits in the Gurney flaps do disturb the two-dimensionality of the wake and reduce the drag by 12 % in the present computation.

## Acknowledgment

This research has been funded by the German National Science Foundation (DFG) within the Special Research Activity (Sonderforschungsbereich) SFB 557, 'Beeinflussung komplexer turbulenter Scherströmungen' at Technical University of Berlin.

## References

- [1] Gruschwitz, E., and Schrenk, O., "Über eine einfache Möglichkeit zur Auftriebserhöhung von Tragflügeln." *Zeitschrift für Flugtechnik und Motorluftschiffahrt*, No. 20, Oktober, pp. 597-601 (1932).
- [2] Abbott, I.H., and von Doenhoff, A.E., "Theory of wing sections", Dover Publications, Inc., New York, (1959)
- [3] zarparka, E.F., "Aircraft and control there of." United States Patent No. 19,412 (1935).
- [4] Liebeck, R.H., "Design of subsonic airfoils for high lift." *Journal of Aircraft*, Vol. 15, No. 9, pp. 547-561 (1978).
- [5] Ross, J.C., Storms, B.L. and Carrannanto, P.G., "Lift-enhancing tabs on multielement airfoils." *Journal of Aircraft*, Vol. 32, No. 3, pp. 649-655 (1995).
- [6] Storms, B.L. and Ross, J.C., "Experimental study of lift-enhancing tabs on a two-element airfoil." *Journal of Aircraft*, Vol. 32, No. 5, pp. 1072-1078 (1995).
- [7] Henne, P.A., "Innovation with computational aerodynamics: The divergent trailing-edge airfoil." *Applied Computational Aerodynamics* (Ed. P.A. Henne). Vol. 125, Progress in Aeronautics, American Institute of Aeronautics and Astronautics, Washington (1990).
- [8] ANON: "Boeing studying 747 variants," *Aviation Week & Space Technology*, June 28, S. 71 (1999).
- [9] Bechert, D.W., Stanewsky, E. and Hage, W., "Windkanalmessungen an einem Transsonik-Flügel mit strömungsbeeinflussenden Maßnahmen. Teil I: Polaren, "DLR-IB 92517-99/B3-1 und Teil II: "Druckverteilungen" DLR-IB 92517-99/B3-2 (1999). Internal Reports
- [10] Sauvage, P., "Étude expérimentale et numérique des écoulements potentiels et visqueux dans le voisinage d'un bord de fuite épais cambré." *Thèse de docteur de L'École Nationale Supérieure de l'Aéronautique et de l'Espace*, Toulouse, No d'ordre: 237. Ph.D. Thesis, École nationale Supérieure de l'aéronautique et de l'espace, Toulouse (1998).
- [11] Kentfield, J.A.C., "Theoretically and experimentally obtained performances of Gurney flap equipped wind turbines." *Wind Engineering*, Vol. 18, No. 2, S. 63-74 (1994).
- [12] Sauvage, P., Pailhas, G. and Coustols, E., "Detailed flow pattern around thick cambered trailing edges." *Proc.: The 7th Asian Congress of Fluid Mechanics*, Chennai (Madras), India, Dec. 8-12 (1997).
- [13] Lee, H.T., Kroo, I.M., "Computational investigation of wings with miniature trailing edge control surfaces." *AIAA 2004-2693* (2004)
- [14] Schatz, M., Günther, B. and Thiele, F., "Computational Modeling of the Unsteady Wake behind Gurney Flaps." *AIAA Paper 2004-2417* (2004).
- [15] Roshko, A.B., "Bluff bodies", *Journal of Aeronautical Sciences*, p. 124 (1955). See also: *NACA Techn. Rpt. 1191* (1954) and *NACA Techn. Notes 2913* (1953) and *3169* (1954).
- [16] Bechert, D.W., Meyer, R. and Hage, W., "Drag reduction of airfoils with miniflaps. Can we learn from dragonflies?" *FLUIDS 2000*, Denver, Co, *AIAA-Paper 2000-2315*. (2000)
- [17] Meyer, R.; Bechert, D. W., and Hage, W., "Drag reduction on Gurney flaps and diverging trailing edges." *CEAS/Dragnet European Drag Reduction Conference 2000*, Potsdam.
- [18] Jeffrey, D., Zhang, X. and Hurst, D.W., "Aerodynamics of Gurney flaps on a single-element high-lift wing." *Journal of Aircraft*, Vol. 37, No. 2, March-April, S. 295-301 (2000).
- [19] Hoerner, S.F., "Fluid dynamic drag." Edition: S.F. Hoerner, 148 Busted Drive, Midland Park, New Jersey, 07432, U.S.A. (1965).
- [20] ALLEN, J.B., "Trailing edge splitter." United States Patent No. 5,265,830; November 30 (1993).
- [21] Meyer, R., "Experimentelle Untersuchungen von Rückstromklappen auf Tragflügeln zur Beeinflussung von Strömungsablösungen." *Ph.D. Thesis*, Technical University Berlin, Mensch & Buchverlag Berlin, (2000).
- [22] Bechert, D. W., "Excitation of instability waves." *Zeitschrift für Flugwissenschaften und Weltraumforschung*, Vol. 9, Nov/Dez, Heft 6, pp. 356 – 361. (1985)
- [23] Huerre, P., and Monkewitz, P., "Absolute and convective instabilities in free shear layers." *Journal of Fluid Mechanics*, Vol. 159, pp. 151 – 168. (1985)
- [24] Koch, W., "Local instability characteristics and frequency determination of self-excited wake flows.", *Journal of Sound and vibration*, Vol.99, pp. 53-83 (1985)

- [25] Rung, T. and Thiele, F., "Computational Modelling of Complex Boundary-Layer Flows." Proc.: 9th Int. Symp. on Transport Phenomena in Thermal-Fluid Engineering, Singapore (1996).
- [26] Schatz, M., "Numerische Simulation der Beeinflussung instationärer Strömungsablösung durch frei bewegliche Rückstromklappen auf Tragflügeln." PH.D Thesis, Technical University Berlin, Mensch & Buchverlag Berlin, (2003).
- [27] Zerihan, J. & Zhang, X.: Aerodynamics of Gurney flaps on a Wing in Ground Effect. AIAA Journal, Vol. 39, No. 5, pp. 772-780 (2001).
- [28] Jeong, J., and Hussain, F., On the identification of a vortex. J. Fluid. Mech. Vol. 285, pp. 69-94 (1995).